International Journal of Engineering Research and Development
e-ISSN: 2278-067X, p-ISSN: 2278-800X, www.ijerd.com
Volume 10, Issue 8 (August 2014), PP.35-50

Improving Transient Stability of Multi-Machine AC/DC Systems via Energy-Function Method

[1]M Shobha, [2]K.Durga Rao, [3]Tegala.Srinivasa Rao,
[1]P.G Student Scholar, [2]Assistant Professor, [3] Associate Professor
[1,2,3]Department of Electrical & Electronics Engineering
[1,2,3]Avanti Institute of Engineering & Technology, Makavaripalem(P),Vishakhapatnam (Dt), Andhra Pradesh, India.

Abstract:- In this paper, the direct method of stability analysis using energy functions is applied for multi-machine AC/DC power systems. The system loads including the terminal characteristics of the DC link are represented as constant current type loads, and their effects on the generators at the internal nodes are obtained as additional bus power injections using the method of distribution factors, thus avoiding transfer conductance terms. Using the centre of angle formulation, a modified form of the energy-function method is used for the swing equations and the DC link dynamical equations to compute the critical clearing time for a given fault. Numerical results of critical clearing time for a single and multi-machine system using the energy-function method agree well with the step-by-step method.

Index Terms:- Direct Current Link, Energy Function, External Control Signal.

I. INTRODUCTION

Direct methods for analyzing power system stability have been applied successfully so far for pure AC systems. The literature on this topic is vast and was summarized in a survey paper by Fouad in 1975. Since 1975, there has been a significant advance in this research area, which has helped to remove the conservative nature of the results associated with this method in the past. Hence, the possibility of using this technique for transient security assessment is now quite good.

Since DC links are now being introduced for economic and other reasons, there is a need to extend the direct method of stability analysis to systems containing such links. It is well known that the quick response of the DC link, as opposed to an AC line combined with an effective control scheme, can enhance transient stability. The degree of transient stability for given fault is either the critical clearing time or the critical energy. The application of the direct method of stability analysis to AC/DC systems is not a routine extension of the method as applied to AC systems. Instead, it requires a different approach based on treating the post fault DC link dynamics as a parameter variation in the swing equations. A simplified first-order model of the DC link controller is proposed, which augments the usual swing equation for the machine. For the multi-machine case, the method using distribution factors is proposed to reflect (at the internal nodes) the terminal characteristics of the DC link and the system loads as additional power injections. This eliminates automatically the problem of transfer conductances in the swing equations. The computational algorithm and results for a multi-machine system are presented.

II. SYSTEM DESCRIPTION

A. *Multi-Machine AC/DC System*

A 3-machine 9-bus system whose single-line diagram is shown in Fig. 3.1 is considered. For details of the AC system date refer to [16]. A DC link is added to the system across Buses 9 and 4. The following parameters are chosen for the DC link:

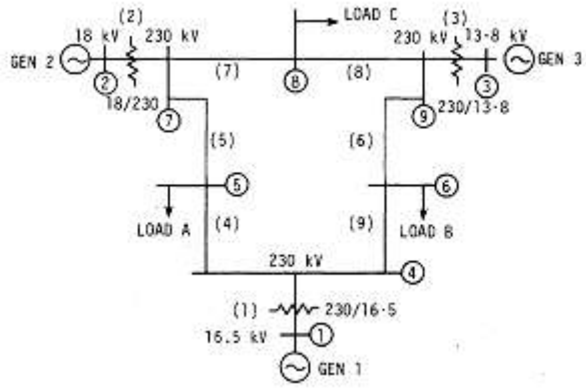

$K_a = 1.0$ pu/rad per sec, $T_{dc} = 0.1$ sec, $P_{ref} = 0.0$

for both prefault and postfault conditions. P_{ref} is assumed to be zero for the sake of convenience. In general, P_{ref} will have different values in the prefault and postfault states, as in the single-machine case; and AC/DC load flow calculations have to be performed for each condition. Maximum $P_{dc} = -2.0$ pu; minimum; $P_{dc} = -2.0$ pu; $q_r = 0.5$. The external control signal (ECS) is chosen to be the difference between the rotor speeds of the generator nearest to the rectifier and inverter terminals, i.e., $u = \omega_3 - \omega_1$.

The extension of the method to multi-machine AC/DC systems involves a new method of handling system loads and DC link characteristics in the swing equations, as well as the use of the potential energy boundary surface method [3, 13] for computing V_{cr}.

TABLE I Comparison of t_{cr} by Energy-Function method and Actual simulation

Postfault Loading on DC Link	t_{cr} by Energy-Function method	t_{cr} by Actual simulation
Case 1: Line (5, 7)	0.181	0.18
Case 2: Line (7, 8)	0.182	0.183
Case 3: Line (4, 6)	0.56	0.57

B. *Representation of the Effect of Loads*

It is well known that the transfer conductances present in the internal bus description using the classical model pose a problem in constructing a valid V-function, as well as in computing t_{cr}. These transfer conductances are mostly due to the system loads being converted to constant impedances and subsequent elimination of the load buses. In the method proposed here, which also applies to the DC link element, the effect of loads is reflected at the internal buses in the form of additional bus power injections.

Consider a power system network consisting of n buses and m generators. The bus admittance matrix Y_{LL} for the transmission network alone, excluding the loads and DC link, is formulated and is thus augmented with the network elements corresponding to direct axis reactances of the m machines. The resulting augmented matrix Y_{Bus} has (n + m) buses altogether, and is represented as

$$Y_{BUS} = \begin{array}{cc} \begin{array}{cc} m & n \end{array} & \\ \begin{bmatrix} Y_{GG} & Y_{GL} \\ Y_{LG} & Y_{LL} \end{bmatrix} & \begin{array}{c} m \\ n \end{array} \end{array} \qquad (1)$$

where Y_{GG}, Y_{GL}, Y_{LG}, and Y_{LL} are submatrices of dimensions (m x m), (m x n), (n x m), and (n x n) respectively. The overall network representation is

$$\begin{bmatrix} \underline{I}_G \\ \underline{I}_L \end{bmatrix} = [Y_{BUS}] \begin{bmatrix} \underline{E}_G \\ \underline{V}_L \end{bmatrix} \qquad (2)$$

where

$$I_G^t = [I_{G1}, I_{G2}, \dots I_{Gm}],\ \ I_L^t = [I_{L1}, I_{L2} \dots . I_{Ln}]$$

I_G and I_L are the current injections at the internal nodes of the generators and the transmission network nodes, respectively; E_G and V_L are the associated voltages. Y_{BUS} is computed for the faulted and postfault conditions by properly taking the corresponding network changes into account. The method of distribution factors are suggested in [15] is now used for reflecting loads at the internal buses. Eliminating V_L from Eq. (3.2), we get

$$V_L = Y_{LL}^{-1} I_L - Y_{LL}^{-1} Y_{LG} E_G \qquad (3)$$

and

$$I_G = [Y'] E_G + [D_L] I_L \qquad (4)$$

where

$$[Y'] = [Y_{GG} - Y_{GL} Y_{LL}^{-1} Y_{LG}]$$

and the distribution factor matrix for loads is given by

$$[D_L] = Y_{GL} Y_{LL}^{-1} \qquad (5)$$

Also, we have

$$I_{Lj} = \frac{-P_{Lj} + j\, Q_{Lj}}{V_{Lj}^{*}} \qquad (6)$$

where P_{Lj} and Q_{Lj} are the active and reactive power components of load at the jth bus. The additional bus power injections at the internal bus of the kth generator (k = 1, 2….m) due to the load at jth bus (j = 1, 2 ….n) is obtained as follows

$$\Delta(P_{kLj} + j\, Q_{kLj}) = -\left(\frac{E_k}{V_{Lj}}\right) d_{kj}^{*}\ (P_{Lj} + j\, Q_{Lj})$$
$$\triangleq (a_{kLj} + j\, b_{kLj})\ (P_{Lj} + j\, Q_{Lj})$$

(7)

Where d_{kj} is the appropriate (k, j) element of $[D_L]$. The following assumption is made regarding the load characteristics: the complex ratio of voltages $\left(E_k / V_{Lj} \right)$ is assumed to be constant, corresponding to the prefault values. This is a deviation from the conventional type of representation of loads as constant impedances. Since only active power is of interest in the swing equation, we get

$$\Delta P_{kLj} = \left(a_{kLj} P_{Lj} - b_{kLj} Q_{Lj}\right) \qquad (8)$$

The effect of all the loads at the internal bus of the kth generator is then obtained as

$$\Delta P_{kL} = \sum_{j=1}^{n} (a_{kLj} P_{Lj} - b_{kLj} Q_{Lj}) \quad k = 1, 2 \dots m \qquad (9)$$

C. *Representation of the Effect of DC Link*

The effect of DC link is represented in a manner similar to that of the loads. For simplicity, we assume only one DC link to be present. The analysis however, easily extends to cases of more than one DC link. In the Y_{BUS} of Eq. (1), all buses except the internal buses of the generators and the bus pair corresponding to the rectifier and inverter terminals of the DC link are eliminated. The reduced network may be represented as

$$\begin{bmatrix} I_G \\ I_D \end{bmatrix} = \begin{bmatrix} Y'_{GG} & Y_{GD} \\ Y_{DG} & Y_{DD} \end{bmatrix} \begin{bmatrix} E_G \\ V_D \end{bmatrix} \quad (10)$$

where

$$I_D^t = [I_r, I_i],\ V_D^t = [V_r, V_i]$$

Subscripts r and I refer to the rectifier and inverter sides, respectively, and $Y'_{GG}, Y_{GD}, Y_{DG}, Y_{DD}$ are submatrices of dimensions (m x m), (m x 2), (2 x m), and (2 x 2), respectively. From Eq. (10), we get

$$V_D = Y_{DD}^{-1} I_D - Y_{DD}^{-1} Y_{DG} E_G \quad (11)$$

and

$$I_G = [Y''] E_G + [D_D] I_D$$

where

$$[Y''] = [Y'_{GG} - Y_{GD} Y_{DD}^{-1} Y_{DG}]$$

and the distribution factor matrix for the DC link is given by

$$[D_D] = Y_{GD} Y_{DD}^{-1} \quad (12)$$

Now, we represent the effect of the DC link currents I_D as additional bus power injections at the internal buses of the generators. We have

$$I_r = \frac{-P_r + j\,Q_r}{V_r^*}$$

and

$$I_i = \frac{-P_i + j\,Q_i}{V_i^*} \quad (13)$$

where

$$P_r = -P_i = P_{dc}$$

and

$$Q_r = Q_i = Q_{dc}$$

It is assumed here that the DC link is lossless and the power factors at the rectifier and inverter stations are equal. P_{dc} and Q_{dc} are the active and reactive power components of the DC link that depend upon the DC link controller dynamics. The effect of the rectifier and inverter ends of the DC link as additional bus power injections at the internal bus of the generator is given by

$$\Delta(P_{kr} + j\,Q_{kr}) = -\left(\frac{E_k}{V_r}\right) d_{kr}^* \,(P_{dc} + j\,Q_{dc})$$
$$\triangleq (a_{kr} + j\,b_{kr})\,(P_{dc} + j\,Q_{dc}) \quad (14)$$

$$\Delta(P_{ki} + j\,Q_{ki}) = -\left(\frac{E_k}{V_i}\right) d_{ki}^* \,(-P_{dc} + j\,Q_{dc})$$
$$\triangleq (a_{ki} + j\,b_{ki})\,(-P_{dc} + j\,Q_{dc}) \quad (15)$$

where d_{kr} and d_{ki} are the appropriate (k, 1) and (k, 2) elements of the matrix $[D_D]$.
From Eqs. (14) and (15), we get

$$\Delta P_{kr} = a_{kr} P_{dc} - b_{kr} Q_{dc} \quad (16)$$

and

$$\Delta P_{ki} = -a_{ki} P_{dc} - b_{ki} Q_{dc}$$

As in the case of the load model representation, here also the ratios $\left({E_k}/{V_r}\right)$ and $\left({E_k}/{V_i}\right)$ are assumed to be constant, corresponding to their prefault values. Since a simple structure is assumed for the DC link controller, the output of which is P_{dc}, let $Q_{dc} = q_r P_{dc}$, where q_r is a constant.

From Eq. (16), we get the total bus power injections at the kth generator due to the DC link as

$$\Delta P_{kD} = \Delta P_{kr} + \Delta P_{ki} = \{(a_{kr} - a_{ki})\} - q_r(b_{kr} + b_{ki})\}P_{dc}$$

$$= c_{kD} P_{dc} \qquad k = 1,2 \ldots .m \qquad (17)$$

Where c_{kD} is the expression in brackets in Eq. (17).

The parameters, a_{kLj}, b_{kLj}, c_{kD} (k = 1, 2…m, j = 1, 2…n),

which reflect the effect of the loads and the DC link, are thus computed for both the faulted and postfault condition. By kron reduction technique, the bus admittance matrix Y_{BUS} is reduced to the internal nodes of the generators for these two conditions.

C. *Inclusion of DC link Dynamics*

A structure similar to that described earlier is assumed for the DC link controller whose equations in terms of P_{dc} are $\dot{P_{dc}} = -\left({1}/{T_{dc}}\right) P_{dc} + {P_{ref}}/{T_{dc}} + \left({K_a}/{T_{dc}}\right) u \qquad (18)$

Where u is the external control signal (ECS) obtained from the AC system quantities, such as the difference in rotor speed of adjacent generators. The DC link dynamics are incorporated into the transient stability analysis in manner similar to the approach described earlier. Also, P_{dc} is constrained to vary with in the specified practical limits. While the faulted system equations are integrated, Eq. (18) also is solved for P_{dc}. At the end each time step, the additional bus power injections at the internal buses of the generators are calculated using Eq. (17). The effect of DC link is thus represented as the term that modifies the power input of the generator.

III. *System Equations*

Under the usual assumptions [1] for the classical model, and following notation in [2], the system equations in the centre-of-angle reference frame are

$$M_k \dot{\widetilde{\omega_k}} = P_k - P_{ek} - \frac{M_k}{M_T} P_{COA}$$

$$\dot{\theta}_k = \widetilde{\omega_k} \qquad k = 1, 2\ldots.m$$

$$(19)$$

where

$$P_k = P_{mk} - \Delta P_{kL} - \Delta P_{kD} - |E_k|^2 G_{kk}$$

$$P_{ek} = \sum_{\substack{j=1\\ \neq k}}^{m} \left(C_{kj} \sin\theta_{jk} + D_{kj} \cos\theta_{kj}\right)$$

$$C_{kj} = |E_k||E_j|B_{kj} \ ; \ D_{kj} = |E_k||E_j|G_{kj}$$

and

$$\theta_k = \delta_k - \delta_o$$

Where δ_o is the centre of angle defined by

$$M_T \delta_o = \sum_{k=1}^{m} M_k \delta_k \ , \ M_T = \sum_{k=1}^{m} M_k$$

The following equation for $\omega_o = \dot{\delta_o}$ is easily derived

$$M_T \dot{\omega}_o = \sum_{k=1}^{m} P_k - 2\sum_{k=1}^{m-1}\sum_{j=k+1}^{m} D_{kj} \cos\theta_{kj}$$
$$\triangleq P_{COA} \qquad (20)$$

In our formulation, since the system loads are not converted into constant impedances, the transfer conductance terms are only due to the transmission lines and hence can be neglected, i.e., $D_{kj} = 0$. If the angle is constant, i.e., $\sum P_k = 0$, then $P_{COA} = 0$ [13]. The postfault SEP is obtained by solving the set of nonlinear equations

$$P_k = P_{ek} \qquad k = 1, 2\ldots..m\text{-}1 \qquad (21)$$

Solution of these power flow equations is discussed extensively in the literature [13, 14].

A. *Transient Energy Function*

The transient energy function used is that given in [2], assuming the damping to be zero

$$V(\underline{\theta}, \underline{\tilde{\omega}}) = \frac{1}{2}\sum_{k=1}^{m} M_k \tilde{\omega}_k^2 - \sum_{k=1}^{m} P_k\left(\theta_k - \theta_k^s\right) - \sum_{k=1}^{m-1}\sum_{j=k+1}^{m} C_{kj}\left(\cos\theta_{kj} - \cos\theta_{kj}^s\right)$$

= kinetic energy (KE) + rotor potential energy (PE) + magnetic potential energy (PE)

$$= V_k(\tilde{\omega}) + V_p(\theta) \qquad (22)$$

where

$V_p(\theta)$ = rotor PE + magnetic PE

B. *Computing V_{cr}*

Following [3], V_{cr} is computed as the value of V_p along the sustained fault trajectory at the instant $\dot{V}_p = 0$. This happens to be a point on the so-called potential energy boundary surface (PEBS) [13]. An assumption is made that the PEBS crossing of the faulted trajectory is a good approximation to the value of V_{cr}, which is the value of V(x) at the controlling UEP [3, 13].

C. *Computational Algorithm*

The algorithm for calculating the critical clearing time based on the proposed method is as follows:

1. Load flow calculation is performed for the prefault AC/DC system.
2. For the faulted and postfault states, the following computations are performed by augmenting the passive network with generator reactance.
   a. The overall Y_{BUS} is computed excluding the loads and the DC link.
   b. The distribution factors due to the system loads and DC link characteristics are computed as explained earlier.
   c. The Y_{BUS} above is reduced to the internal buses of generators by eliminating all other buses. In doing so, the transmission line resistance is neglected.
3. The postfault SEP is computed by solving the nonlinear Eq. (21).
4. The faulted Eqs. (18) & (19) are numerically integrated to obtain values of $\theta, \tilde{\omega}, P_{dc}$ at $t = \Delta t$. At the end of the integration interval, the following computations are done.
   a. P_{dc} obtained from Eq. (18) is used in updating the bus power injections for both faulted and postfault states.
   b. P_k is accordingly modified in Eq. (19), and the new postfault SEP θ^s is computed by solving Eq. (21).
   c. Using the updated values of θ^s, the V-function in (22), as well as V_p and $\dot{V}_p$ are calculated.

d. The integration is now continued for the faulted Eqs. (18) and (19) and steps (a) - (c) are repeated at $t = 2\Delta t$. For the sustained fault trajectory, this is continued until $\dot{V}_p$ changes sign from positive to negative. The value of V_p at this instant is an estimate of V_{cr}.

5. Using this value of V_{cr}, the integration of the faulted equations is carried out and t_{cr} is reached when $V(\theta, \tilde{\omega}) = V_{cr}$. Steps 4(a) and (b) are incorporated during the integration.

IV. SIMULATION RESULTS AND DISCUSSIONS

Case 1: Line (5, 7), t = 0.18sec, Unstable without HVDC

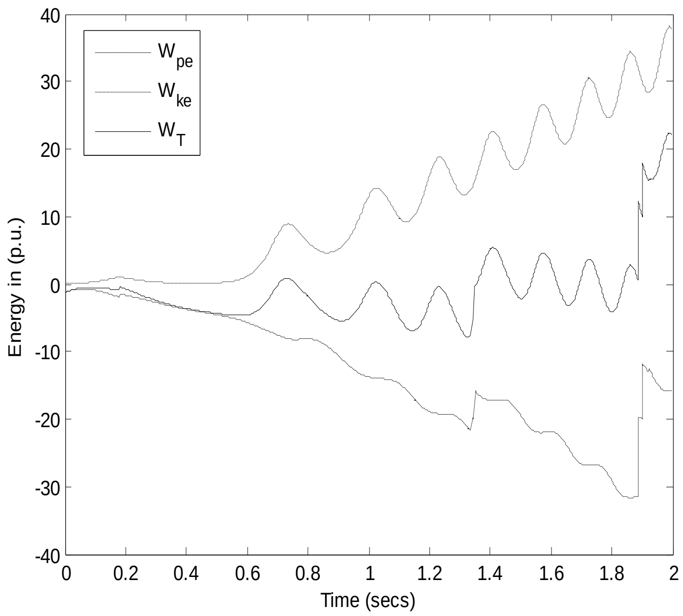

Figure. 4.2. Variation of Energy with time without HVDC

Case1: line (5, 7), t = 0.18sec, Stable with HVDC

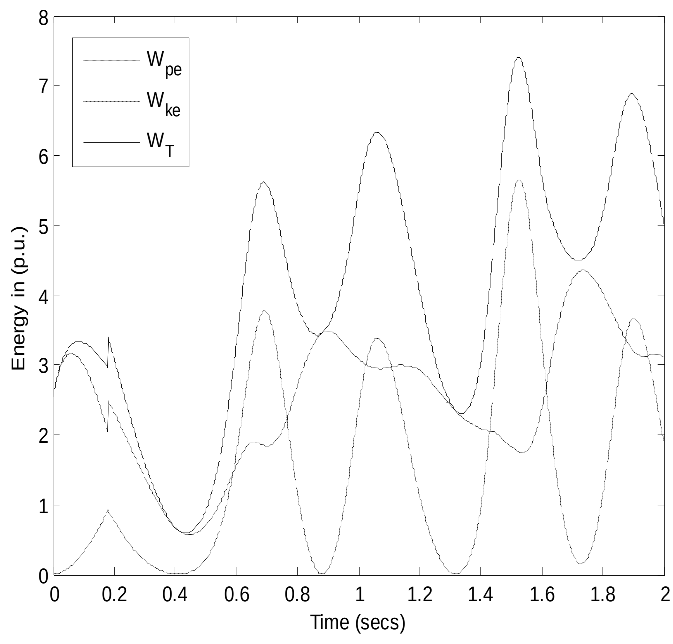

Figure. 4.3. Variation of Energy with time with HVDC

Case1: line (5, 7), t = 0.18sec

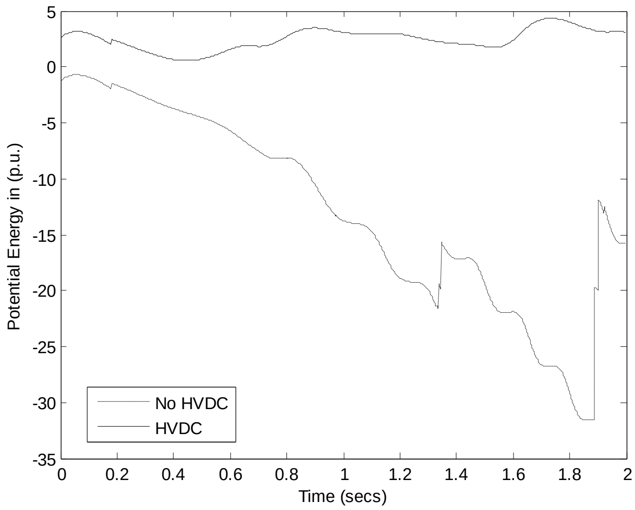

Figure. 4.4. Variation of potential energy with time

<u>Case1</u>: line (5, 7), t = 0.18sec

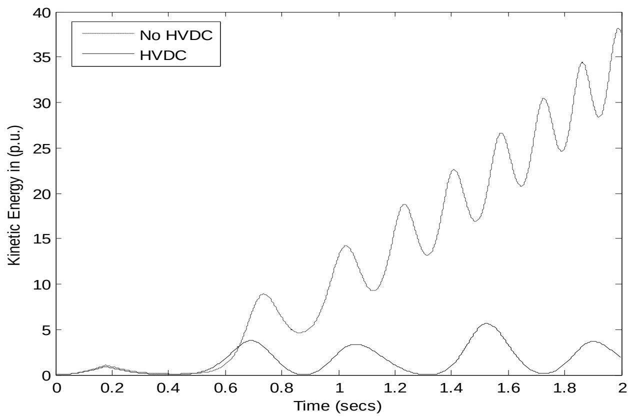

Figure. 4.5. Variation of kinetic energy with time

<u>Case1</u>: line (5, 7), t = 0.18sec

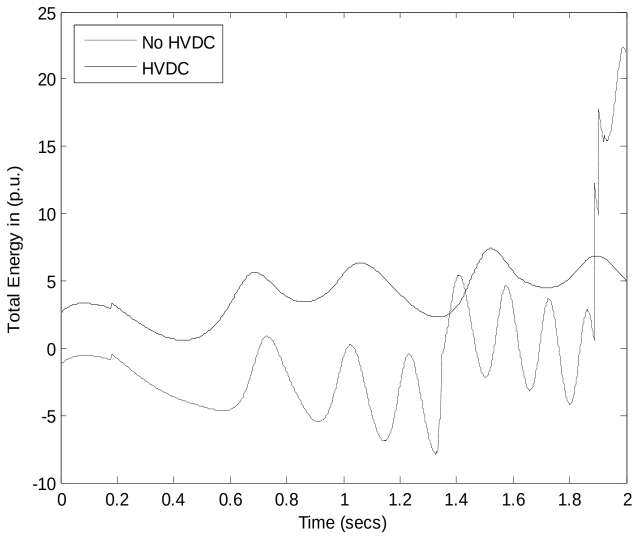

Figure. 4.6. Variation of Total energy with time

<u>Case1</u>: line (5, 7), t = 0.181sec of Machine-1

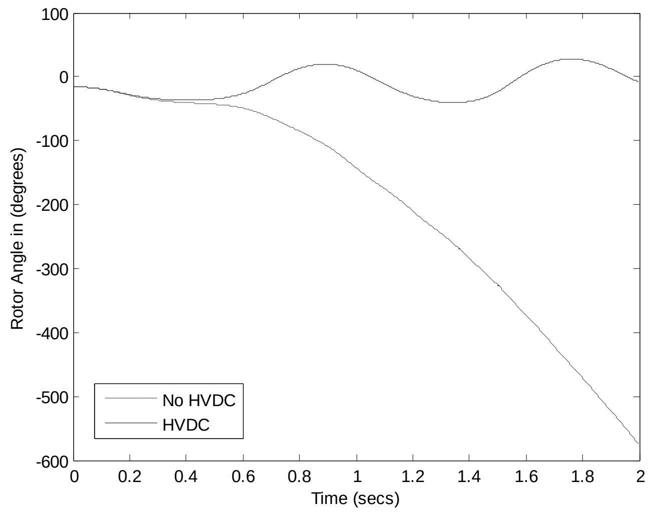

Figure. 4.7. Variation of Rotor angle with time

<u>Case1</u>: line (5, 7), t = 0.181sec of Machine-2

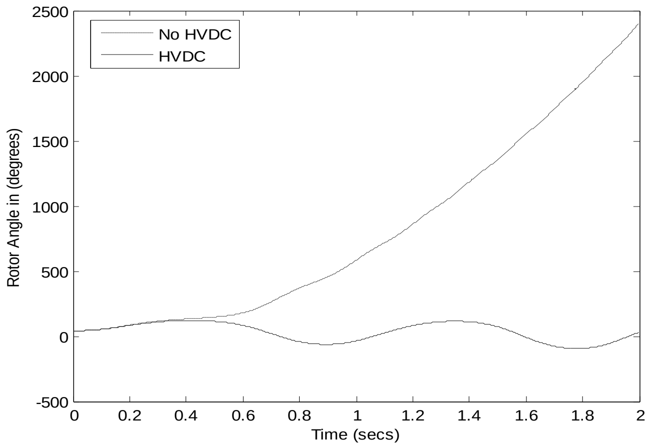

Figure. 4.8. Variation of Rotor angle with time

<u>Case1</u>: line (5, 7), t = 0.181sec of Machine-3

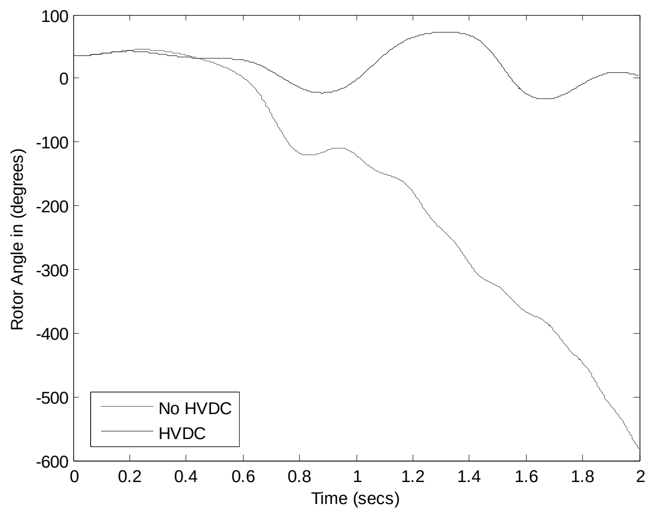

Figure. 4.9. Variation of Rotor angle with time

<u>Case 2</u>: Line (7, 8), t = 0.182sec, Unstable without HVDC

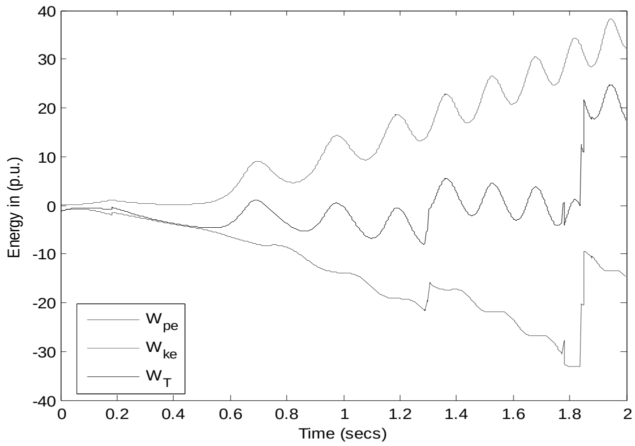

Figure. 4.10. Variation of Energy with time without HVDC

<u>Case2</u>: line (7, 8), t = 0.182sec, Stable with HVDC

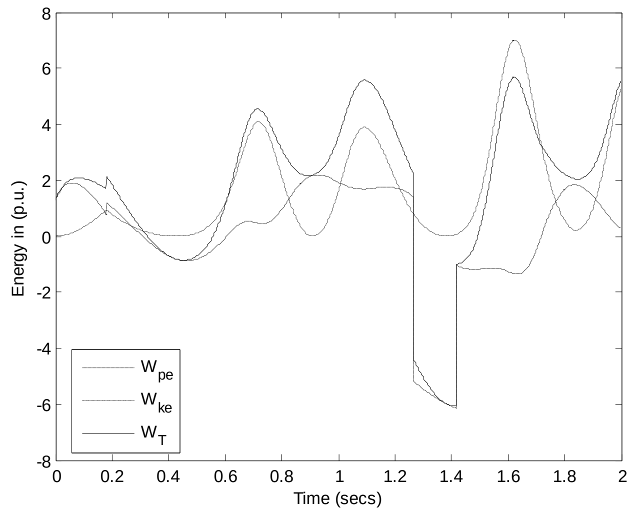

Figure. 4.11. Variation of Energy with time with HVDC

<u>Case2</u>: line (7, 8), t = 0.182sec

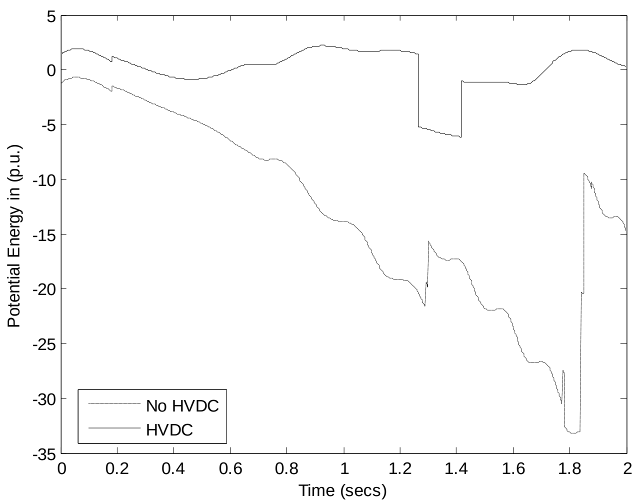

Figure. 4.12. Variation of potential energy with time

Case2: line (7, 8), t = 0.182sec

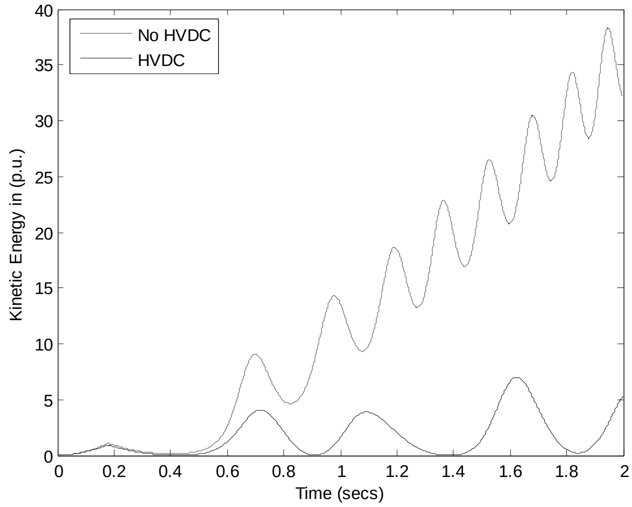

Figure. 4.13. Variation of kinetic energy with time

Case2: line (7, 8), t = 0.182sec

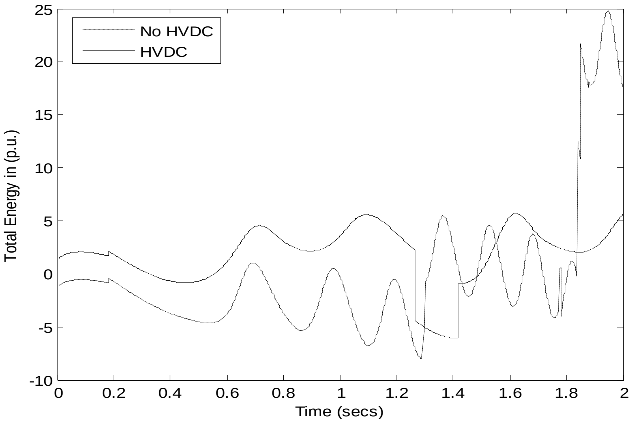

Figure. 4.14. Variation of Total energy with time

Case2: line (7, 8), t = 0.183sec of Machine-1

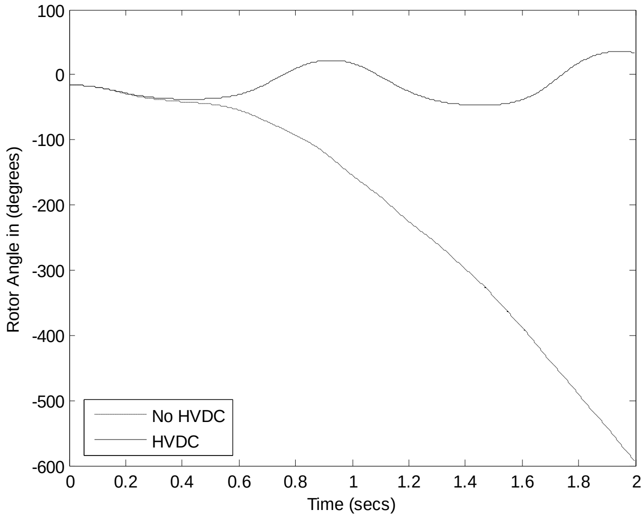

Figure. 4.15. Variation of Rotor angle with time

<u>Case2</u>: line (7, 8), t = 0.183sec of Machine-2

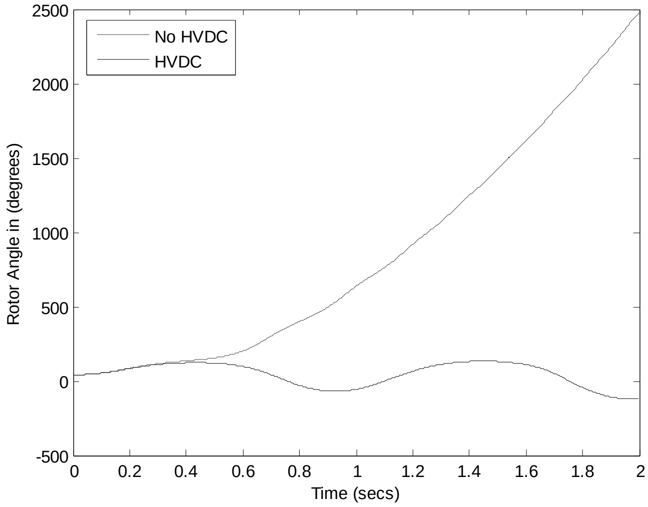

Figure. 4.16. Variation of Rotor angle with time

<u>Case2</u>: line (7, 8), t = 0.183sec of Machine-3

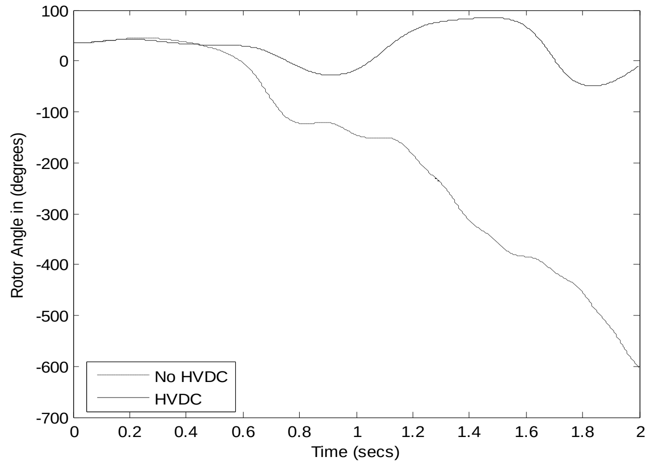

Figure. 4.17. Variation of Rotor angle with time

<u>Case 3</u>: Line (4, 6), t = 0.56sec, Unstable without HVDC

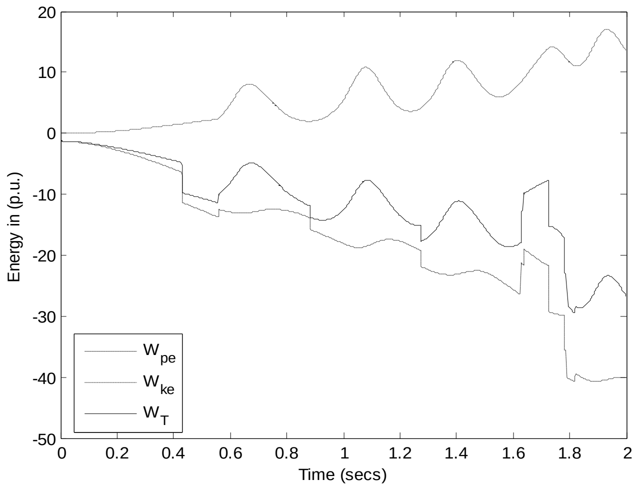

Figure. 4.18. Variation of Energy with time without HVDC

<u>Case 3</u>: Line (4, 6), t = 0.56sec, Unstable without HVDC

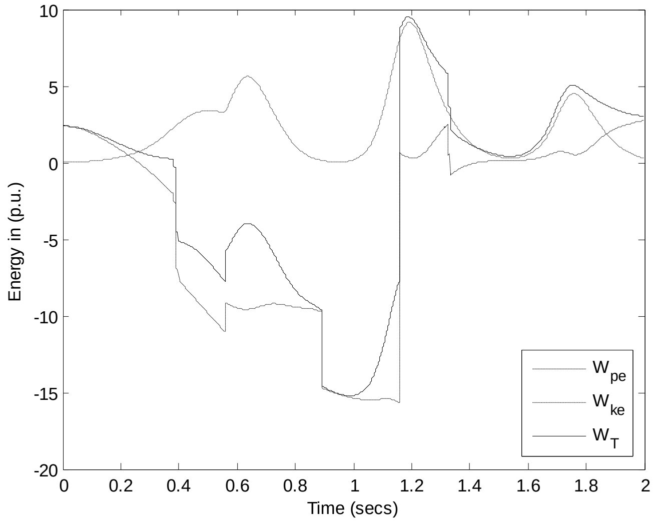

Figure. 4.19. Variation of Energy with time with HVDC

<u>Case 3</u>: Line (4, 6), t = 0.56sec

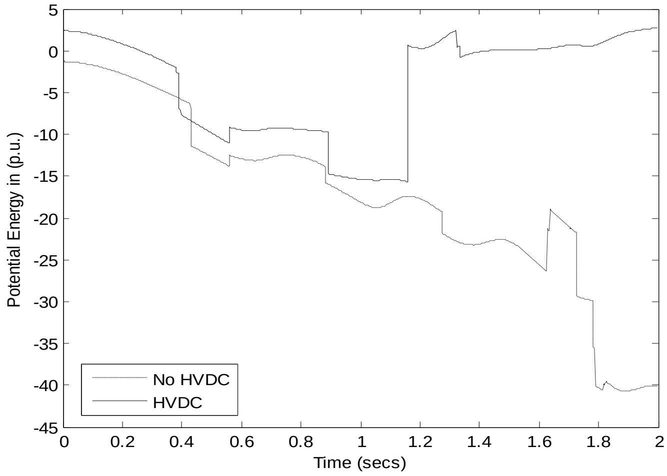

Figure. 4.20. Variation of Potential energy with time

<u>Case 3</u>: Line (4, 6), t = 0.56sec

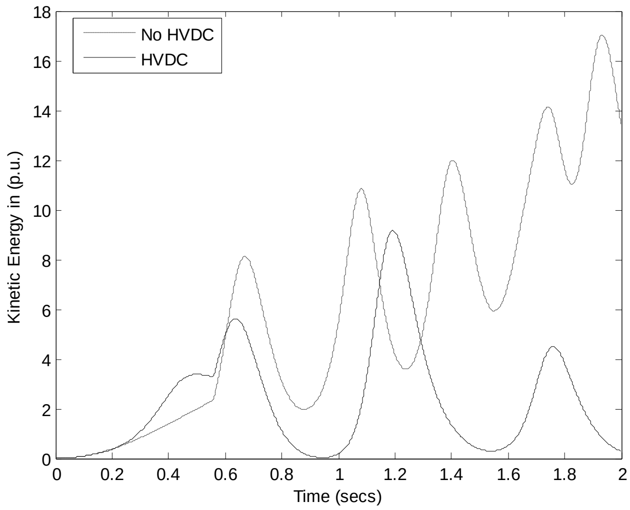

Figure. 4.21. Variation of kinetic energy with time

<u>Case 3</u>: Line (4, 6), t = 0.56sec

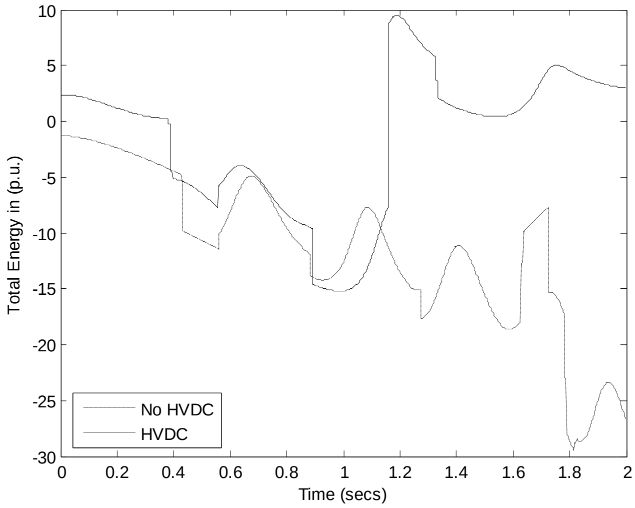

Figure. 4.22. Variation of Total energy with time

<u>Case 3</u>: Line (4, 6), t = 0.57sec of Machine-1

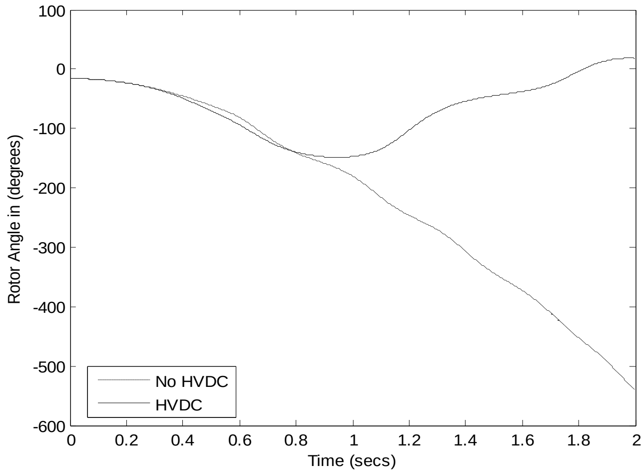

Figure. 4.23. Variation of Rotor angle with time

<u>Case 3</u>: Line (4, 6), t = 0.57sec of Machine-2

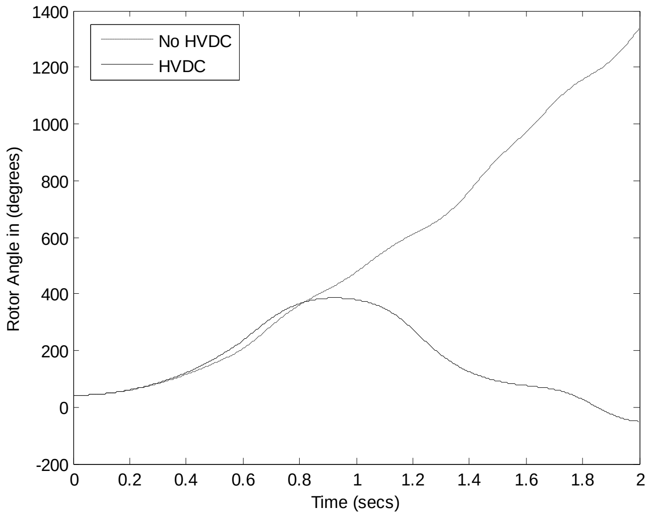

Figure. 4.24. Variation of Rotor angle with time

<u>Case 3</u>: Line (4, 6), t = 0.57sec of Machine-3

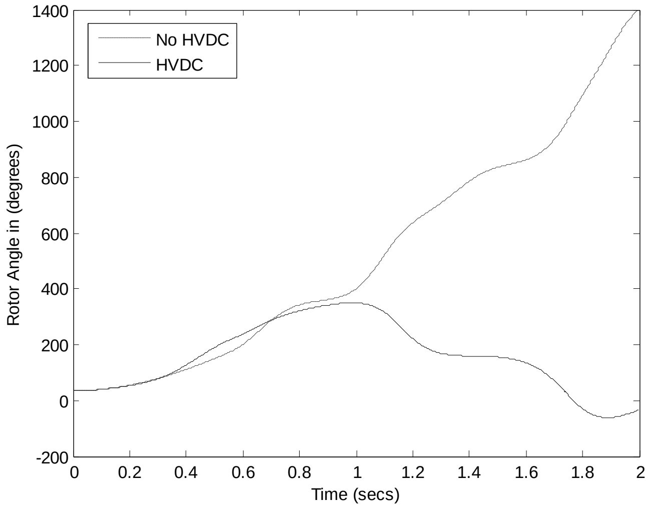

Figure. 4.25. Variation of Rotor angle with time

V. CONCLUSION

In this paper, a technique is proposed for applying to the direct method of stability analysis to multi-machine AC/DC systems. A new method of handling transfer conductances is presented that is also useful in representing the DC link characteristics in the swing equations. The centre-of-angle formulation is used. A 3-machine, nine-bus system illustrates the validity of the method and the effects of the DC link in improving transient stability. Three case studies have been done and the computational algorithm and simulation results are presented.

VI. APPENDIX

Generator data: Base 100MVA
Gen 1: 16.5/230 kv
Gen 2: 18/230 kv
Gen 3: 13.8/230 kv
K_a = 1.0 pu/rad per sec
T_{dc} = 0.1 sec
P_{ref} = 0.0
Maximum P_{dc} = 2.0 pu
Minimum P_{dc} = -2.0 pu
q_r = 0.5

REFERENCES

[1]. A.A. Fouad, "Stability Theory—Criteria for Transient Stability." Proceedings of the Engineering Foundation Conference on System Engineering on Power, Henniker, New Hampshire, Publication No. CONF-750867, pp. 421-450, 1975.

[2]. T. Athay, R. Podmore, and S. Virmani, "A Practical Method for Direct Analysis of Transient Stability." IEEE Transactions on Power Apparatus and System, vol. PAS-98, No. 2, pp. 573-584, 1979.

[3]. N. Kakimoto, Y. Ohsawa, and M. Hayashi, "Transient Stability Analysis of Electric Power System via Lure' Type Lyapunov Function, Parts I and II." Transactions of IEEE of Japan, vol. 98, No. 5/6, May/June 1978.

[4]. M. Ribbens Pavella, Lj T. Gruijc, T. Sabatel, and A. Bouffioux, "Direct Methods of Stability Analysis of Large Scale Power Systems." Proceedings of the IFAC Symposium on Computer Applications in Large-Scale Power Systems, New Delhi, India, vol. II, pp. 168-175, August 1979.

[5]. A. A. Fouad, and S. E. Stanton, "Transient Stability of a Machine Power System, Parts I and II." Papers No. 81 WM 078-5 and 81 WM 079-3, IEEE Winter Power Meeting, Atlanta, Georgia, Feb. 1-6, 1981.

[6]. E. Uhlmann, "Stabilization of an AC link by a Parallel DC link." Direct Current, vol. 12, No. 8, pp. 89-94, 1964.

[7]. H. A. Peterson, and P. C. Krause, "Damping of Power Swings in a Parallel AC and DC system." IEEE Transactions on Power Apparatus and Systems, vol. PAS-85, pp. 1231-1239, 1966.

[8]. W. K. Marshall, K. R. Padiyar, L. M. Denton, W. J. Smolinski, and E. F. Hill, " A Simplified HVDC Link representation for Stability Studies." Paper C-74-434-7, IEEE Summer Power Meeting, July 1974.

[9]. M. A, Pai, M. A. Mohan, and J. G. Rao, "Power System Transient Stability Region Using Popov's Method." IEEE Transactions on Power Apparatus and Systems, vol. PAS-89, No. 5, pp. 788-794, May/June 1970.

[10]. J. L. Willems, and J. C. Willems, "The Application of Lyapunov Methods to the Computation of Stability Regions of Multi-Machine Power Systems, IEEE Transactions on Power Apparatus and Systems, vol. Pas-89, No. 5, pp. 795-801, May/June 1970.

[11]. J. L. Abatut and J. Fantin, "Etude de la Stabilite Transitoire dans un Systeme de Puissance Influence des Parametres." Automatic Control Theory and Application, vol. 2, pp. 14-18, 1973.

[12]. H. Sasaki, "An Approximate Incorporation of Field Flux Decay into Transient Stability Analysis of Multi-Machine Power Systems by the Second Method of Lyapunov." IEEE Transactions on Power Apparatus and Systems, vol. PAS-98, No. 2, pp. 473-483, March/ April 1979.

[13]. T. Athay, V. R. Sherkey, R. Podmore, S. Virmani, and C. Puech, "Transient Energy Stability Analysis." Systems Engineering for Power: Emergency Operating State Control- -Section IV, U.S. Department of Energy Publication No. CONF-790904-PL, October 1979.

[14]. A. H. El-Abiad, and K. Nagappan, "Transient Stability Region of Multi-Machine Power Systems." IEEE Transactions on Power Apparatus and Systems, vol. PAS-85, pp. 169-179, February 1966.

[15]. W. F. Tinney, and W. L. Powell, "The REI Approach to Power Network Equivalents." 1977 PICA Conference, Toronto, Canada, May 1977.

[16]. P. M. Anderson, and A. A. Fouad, Power System Control and Stability. Ames, Iowa State University Press, 1977.

[17]. J. J. Dougherty, and T. Hillesland, "Power System Stability Considerations with Dynamically Responsive DC Transmission Lines." IEEE Transactions on Power Apparatus and Systems, vol. PAS-95, pp. 536-541, March/April 1976.

[18]. J. Reeve, "Multiterminal HVDC Power Systems." IEEE Transactions on Power Apparatus and Systems, vol. PAS-99, No. 2, pp. 729-737, March/April 1980.